IJE TRANSACTIONS B: Applications Vol. 36 No. 11, (November 2023) 1972-1981

International Journal of Engineering

Journal Homepage: www.ije.ir

Investigation of Shell Side Overall Performance of a Novel Shell-and-Double-Concentric –tube Heat Exchanger with Simple and Perforated Helical Baffles

H. O. Sayevand*, S. Khorshidi, B. Keshavarzian

Mechanical Engineering Department, Bu-Ali Sina University, Hamedan, Iran

PAPER INFO

Paper history:
Received 27 May 2023
Received in revised form 06 August 2023
Accepted 20 August 2023

Keywords:
Heat Exchanger
Shell-and-double-concentric-tube
Perforated
Helical Baffles

ABSTRACT

In this study, the overall performance of a heat exchanger shell-and-double-concentric-tube with simple and perforated helical baffles is investigated in the shell side of the heat exchanger using ANSYS FLUENT 19.2. A comparison between the shell-side with simple helical baffles of the heat exchanger (SHB-SDCTHEX) and the one with perforated helical baffles (PHB-SDCTHEX) using numerous mass flow rates is carried out. For the perforated helical baffles heat transfer rate Q, thermo-hydraulic performance $Q/\Delta P$ and effectiveness ε are around 26.7%, 55.5% and 26.6% higher than the same parameters for the simple helical baffles of the heat exchanger, respectively. It is also observed that the flow and temperature distribution for the perforated helical baffles are more uniform with higher flow turbulence than the simple helical baffles of the heat exchanger. So, the perforated helical baffles could be a better choice for the designers and manufacturers with respect to the simple helical baffles of the heat exchanger.

doi: *10.5829/ije.2023.36.11b.03*

NOMENCLATURE

A	Heat transfer area (m^2)
c_p	Specific heat (J/kg.K)
d_2	Inside diameter of inner tube (mm)
d_1	The outside diameter of inner tube (mm)
D_2	Inside diameter of the outer tube (mm)
D_1	Outside diameter of the outer tube (mm)
h	Heat transfer coefficient ($W/m^2.K$)
L	Length (m)
k	Turbulent kinetic energy (m^2/s^2)
m	Mass flow rate (kg/s)
M	mesh used
N	Number
Q	Heat transfer rate (W)
Δp	Pressure drop (pa)
T	Temperature (K)
ΔT_m	Logarithmic temperature difference (K)
U	Overall heat transfer coefficient ($W/m^2.K$)
V	Velocity (m/s)
Greek symbol	
μ	Dynamic viscosity (kg/m.s)
υ	Kinematic viscosity (m^2/s)
υ_t	Turbulent Kinematic viscosity (m^2/s)
λ	Thermal conductivity (W/m.K)
ρ	Density (kg/m^3)
σ_k	Prandtl number of k
σ_ε	Prandtl number of ε
Γ	Generalized diffusion coefficient
ε	Dissipation rate of turbulence (m^2/s^3)
ε	effectiveness
Abbreviations	
CFD	Computational fluid dynamics
HE	Heat exchanger
STHEX	Shell-and-tube HE
SDCTHEX	Shell-and-double-concentric-tube HE
SHB- SDCTHEX	Shell-and-double-concentric-tube HE with simple helical baffle
S&T	Shell and tube
PHB-SDCTHEX	Shell-and-double-concentric-tube HE with perforated helical baffle
Subscripts	
av	Average
a	Annulus
h	Hydraulic
inner	Hydraulic
i	Inner
in	Inlet
min	Minimum
max	Maximum
out	Outlet
s	Shell-side
t	Tube-side
w	Wall-side

*Corresponding Author Email: hsayeh@basu.ac.ir (H. O. Sayevand)

Please cite this article as: H. O. Sayevand, S. Khorshidi, B. Keshavarzian, Investigation of Shell Side Overall Performance of a Novel Shell-and-Double-Concentric –tube Heat Exchanger with Simple and Perforated Helical Baffles, ***International Journal of Engineering, Transactions B: Applications***, Vol. 36, No. 11, (2023), 1972-1981

1. INTRODUCTION

HEs are one of the principal supplies utilized extensively in chemical industry, steam production, and oil refineries. Among all groups of heat exchangers (HE), the shell and tube (S&T) one has had many applications in heat transfer technology [1-4] and is the most appropriate for higher pressure operations. Many investigations have been engaged to improve S&T HE efficiency and numerous approaches have been adopted for this purpose. One of the most important concerns of the industry has always been increasing heat transfer for various uses, and efforts have been made in this field. For example, the use of porous materials, Induced vibrations, nano-fluids, and nanoparticles in fluid have always been investigated to increase heat transfer in heat exchangers and energy storage systems [5-14]. One of these practical approaches is using various baffles on shell-side to change the flow direction and mix the fluid. So far, researchers have investigated several baffles with diverse formations such as segmental and double segmental baffles [15, 16], ring supports [17], helical baffles [18-27] and rod baffles [28-30] using empirical, numerical and analytical approaches. Hosseinzade et al. [31] investigated the effect of two different fins (longitudinal-tree like) on energy storage using the phase changer method. Using the analytical method can reveal the possible defects in S&T design, but it cannot identify where these faults are [15]. CFD (numerical approach) can conceive the distribution of temperature and fluid flow particularly on the shell-side, which can facilitate estimating the weak points, and so denoting the possible rectifications to be applied for efficiency improvement [15]. In addition, economic efficiency, flow field observation, and time expenditure are some privileges of the numerical approach concerning to the empirical approach [32]. As a result, several numerical investigations have been accomplished on S&T HE. Bougriou and Baadache [33] researched on SDCTHEX. Difference between the SDCTHEX and classical S&T HE is that the S&T HE tube has been replaced by the double concentric tube. As a result of adding the inner tube, the SDCTHEX has a larger heat transfer area than the S&T HE. Subsequently, increasing the area of heat transfer would make the HE more compact for a specific amount of heat transfer. This causes reducing the cost of manufacturing and the dimensions of the device.

Shahril et al. [15] studied the SDCTHEX and S&T HE with segmental baffle and made a comprehensive comparison of both types of the HE. They revealed that a SDCTHEX is equivalent to a S&T HE if the S&T HE is used with two tube passes and one shell, where hot oil flows in the inner tube and shell. In contrast, water flows in the annulus they found that the average of $Q/\Delta P$ parameter for SDCTHEX is around 343% higher than that of the S&T HE. They realized that apart from their advantages, using the segmental baffles has also some disadvantages as follows: (1) higher pressure drop in shell-side because of abrupt constriction and distension of flow and severity of flow contact with shell wall and baffles, (2) creation of dead spots in the junction of the segmental baffle and the shell resulting in low heat transfer coefficient, (3) They found that the average of $Q/\Delta P$ parameter for SDCTHEX is around 343% higher than that of the S&T HE. In recent years, to crack these weaknesses, rod baffles, deflecting baffles, and disk-and-doughnut baffles have been evolved [1]. But, none of these baffles could eliminate the defects listed above. Instead, baffles with helical shapes could be a suitable option to substitute segmental baffles by avoiding the cons cited above [34].

Finding a suitable design in heat exchangers to increase thermal efficiency along with reducing pressure drop has always been the focus of the industry. Therefore, a lot of research has been done on the types of fins and even their arrangement and this research has always continued. Helical fins are one of the types of fins used in shell-tube heat exchangers in order to increase heat transfer. Nevertheless, helical baffles cannot thoroughly flow the fluid uniformly across the shell-side as this issue can cause a low heat transfer coefficient in some spots of the shell-side. In this study, the perforated helical baffle is provided to resolve this issue. It is made by creating orifices on the simple helical baffle to allow the flow to cross through these orifices. This new type of fin, by affecting the amount of fluid flow turbulence, makes the thermal efficiency and performance of perforated fins much higher than its simple state, and the pressure drop of the fluid flow is also lower. This issue can be very important for the construction of shell and tube heat exchangers. Due to the fact that higher efficiency and smaller dimensions with lower pressure drop will be the result of using this type of fin.

2. DESCRIPTION OF THE SYSTEM

The perspective views of the SHB-SDCTHEX and the PHB-SDCTHEX are depicted in Figure 1. The length of the HE for the shell and tubes is 1270 mm and 1286 mm, respectively. The internal shell diameter is 337 mm with 55 concentric tubes placed inside the shell in a staggered arrangement. For the inner tubes of SHB-SDCTHEX and PHB-SDCTHEX the internal and external diameters are 8 mm and 12 mm, and 20 mm and 24 mm for the outer tubes, respectively. Also, the diameter of the orifices in the perforated helical baffle is 8 mm. The AISI 1042-annealed steel is adopted as the material for the baffles and tubes, by density $= 7840\ \mathrm{kg/m^3}$, specific heat $c_p = 460\ \mathrm{J/kg.K}$ and thermal conductivity $\lambda = 50\ \mathrm{w/m.K}$

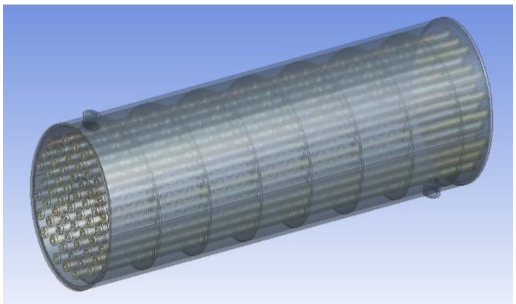

(a) SHB-SDCTHEX

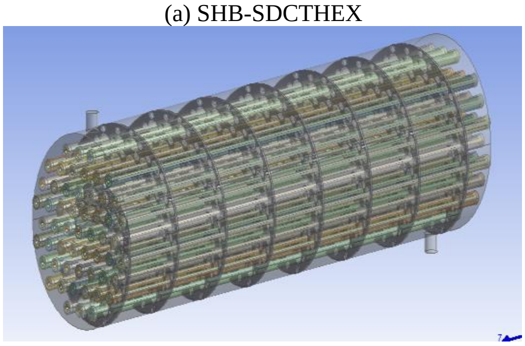

(b) PHB-SDCTHEX

Figure 1. Perspective views of the SHB-SDCTHEX and PHB-SDCTHEX

[20]. The thickness and the section angle for both baffles are 5 mm and 20°, respectively. Also, the working fluids are engine oil and water. Engine oil flows inside the shell and the inner tube as the hot fluid, while water flows inside the annulus as the cold fluid. The properties of the working fluids are described in ANSYS FLUENT 19.2 using the piecewise-linear function of temperature and also can be obtained from literature [35].

3. NUMERICAL ANALYSIS:

3. 1. Model Development

The equations of the momentum, continuity, energy, k and ε are shown as below. The steady state, incompressible and turbulent flow assumptions are engaged [15]:

Continuity equation:

$$\frac{\partial u_i}{\partial x_i} = 0 \tag{1}$$

Momentum equation:

$$\frac{\partial u_i u_j}{\partial x_i} = -\frac{1}{\rho}\frac{\partial \rho}{\partial x_i} + \frac{\partial}{\partial x_j}((\upsilon + \upsilon_t)(\frac{\partial u_j}{\partial x_i} + \frac{\partial u_i}{\partial x_j})) \tag{2}$$

Energy equation:

$$\frac{\partial u_i T}{\partial x_i} = \frac{\partial}{\partial x_i}((\frac{\upsilon}{pr} + \frac{\upsilon_t}{pr_t})\frac{\partial T}{\partial x_i}) \tag{3}$$

Turbulent kinetic energy k equation:

$$\frac{\partial u_i k}{\partial x_i} = \frac{\partial}{\partial x_i}\left(\left(\upsilon + \frac{\upsilon_t}{\sigma_k}\right)\frac{\partial k}{\partial x_i}\right) + \Gamma - \varepsilon \tag{4}$$

Turbulent energy dissipation ε equation:

$$\frac{\partial u_i \varepsilon}{\partial x_i} = \frac{\partial}{\partial x_i}\left(\left(\upsilon + \frac{\upsilon_t}{\sigma_\varepsilon}\right)\frac{\partial \varepsilon}{\partial x_i}\right) - C_2\frac{\varepsilon^2}{k + \sqrt{\upsilon\varepsilon}} \tag{5}$$

where:

$$\Gamma = -\overline{u_i}\,\overline{u_j}\frac{\partial u_i}{\partial x_j} = \upsilon_t(\frac{\partial u_i}{\partial x_j} + \frac{\partial u_j}{\partial x_i})\frac{\partial u_i}{\partial u_i}\ ,\ \upsilon_t = C_\mu\frac{k^2}{\varepsilon} \tag{6}$$

The $k - \varepsilon$ turbulence model practical constants are: C_2 = 1.2, σ_k = 1.0, σ_ε = 1.2**.** Also, C_μ has a constant value for a high Reynolds number. However, C_μ was considered a function of the strain and rotation rate [36].

3. 2. Boundary Conditions and Numerical Approach

Numerical analysis is accomplished by applying CFD software ANSYS FLUENT 19.2**.** The working fluids for both samples of the HE SHB-SDCTHEX and PHB-SDCTHEX are engine oil and water. The engine oil flows in the shell and the inner tubes with the same m_s , and water is allocated as working fluid in the annulus.

The boundary conditions are explained for the SHB-SDCTHEX and the PHB-SDCTHEX as follows:

(1) The shell-side inlet:
m_s = 20 (kg/s), $T_{s,in}$ = 393 (°k), $V_{s,in}$ = 68.26 (m/**s**).

(2) The inner tube side inlet:
m_t = 20 (kg/s), $T_{t,in}$ = 393 (°k).

(3) The annulus side inlet:
m_a = 10.14 (kg/s), $T_{t,in}$ = 293 (°k).

(4) The outlet boundary condition: pressure outlet.

(5) Wall boundary conditions: non-slip boundary, the coupled thermal boundary is applied for the wall of the tubes and baffles. Also, adiabatic condition is used for thermal boundary of the shell wall.

Pressure-based and double-precision solver is used here. For the near wall zone, the realizable $k - \varepsilon$ and scalable wall function is employed for all simulations. The SIMPLE and the second-order-upwind difference scheme are set in the simulations.

Simulations are carried out under the following assumptions:

(1) The fluid properties of the working are constant.

(2) The gravity effect is ignored.

(3) Thermal radiation is negligible.

Data reduction:

Heat transfer balance for the shell and the inner tube is gained:

$$Q_a = Q_s + Q_i \tag{7}$$

where:

$$\begin{aligned} Q_a &= m_a c_{pa}(T_{(a,out)} - T_{(a,in)}) \\ Q_s &= m_s c_{ps}(T_{(s,in)} - T_{(s,out)}) \\ Q_i &= m_i c_{pi}(T_{(i,in)} - T_{(i,out)}) \end{aligned} \tag{8}$$

The mean heat transfer rate (Q_{av}) is defined by:

$Q_{av} = (Q_a + Q_{s,i})/2$

Where $Q_{s,i} = Q_s + Q_i$

Due to the counter flow of the water in the annulus side, the logarithmic average temperature difference between the shell and the annulus is obtained by:

$$\Delta T_{m_{1,2}} = \frac{(T_{s,in}-T_{a,out})-(T_{s,out}-T_{a,in})}{ln\frac{(T_{s,in}-T_{a,out})}{(T_{s,out}-T_{a,in})}} \quad (9)$$

The total heat transfer coefficient from the shell side to the annulus side is obtained by:

$$U_{1,2} = {}^{Q_s}/_{N_a}\, \pi D_1 L_a F \Delta T_{m_{1,2}} \quad (10)$$

The convection heat transfer coefficient of the shell side is obtained from:

$$h_s = \frac{1}{\frac{1}{U_{1,2}} - \frac{1}{h}\frac{D_1}{D_2} - \frac{D_1}{2\lambda_a} ln\frac{D_1}{D_2}} \quad (11)$$

3. 3. Validation 3D geometry configurations of the HE were constructed using the Solid Works software. As shown in Figure 2, the computational mesh, by the workbench in ANSYS FLUENT, is generated with an unstructured grid. For grid study of the SHB-SDCTHEX model, five various meshes (M1: 6954315, M2: 11753218, M3: 12853619, M4: 13998340, and M5: 15697562 elements) were considered. In order to choose the best mesh that is favorable for the problem in terms of economy and accuracy of the results, by comparing the pressure drop and the heat transfer coefficient obtained for the meshes. The M4 was considered for further calculations (it should be noted that the residual squared errors for the flow field and pressure is considered 10^{-5} for convergence). Comparing the results obtained in this research with the results of the Bell-Delaware approach described by Shahril et al. [15] is used for the heat transfer coefficient of shell side and the shell side pressure drop for the SHB-SDCTHEX and PHB-SDCTHEX in Figures 3 and 4. The maximum difference

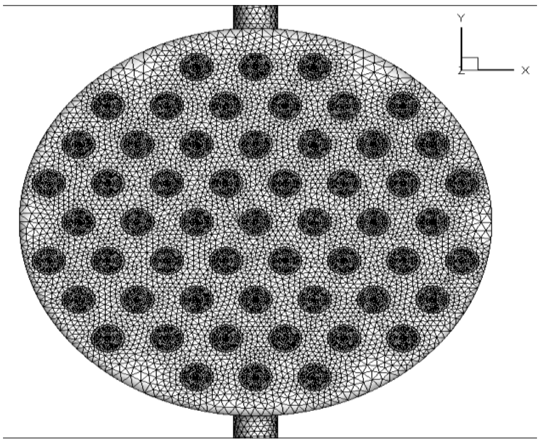

(a) front view

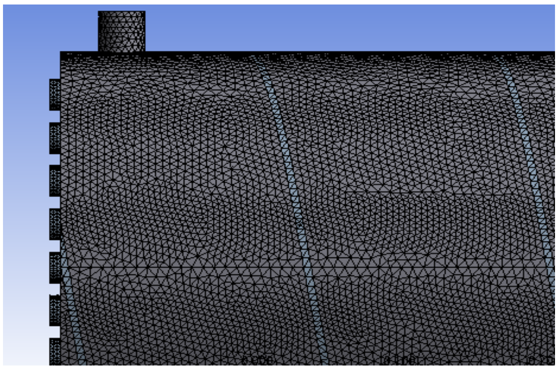

(b) side view

Figure 2. Local Views of the grid system for SHB-SDCTHEX and PHB-SDCTHEX.

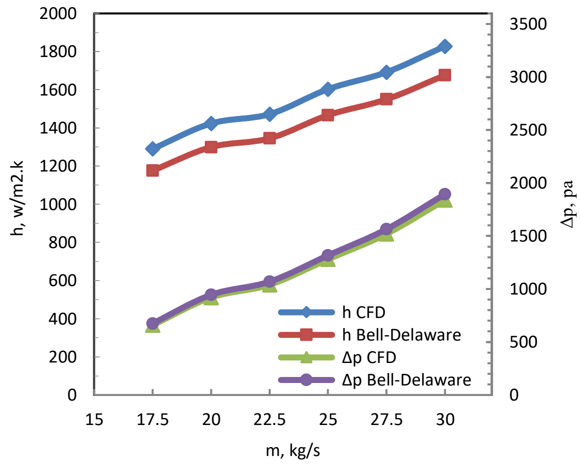

Figure 3. Comparison between the numerical calculations and the Bell-Delaware approach for the shell side of the SHB-SDCTHEX

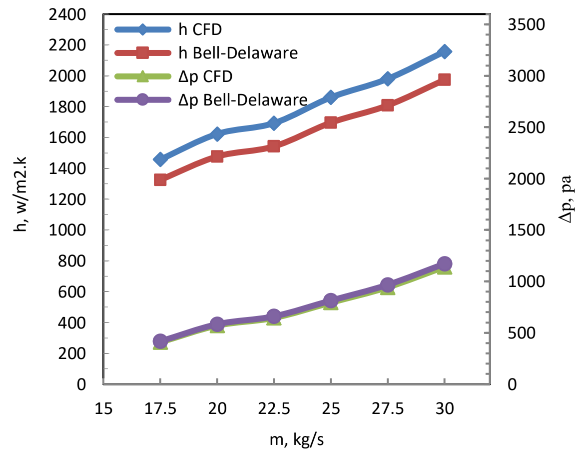

Figure 4. Comparison between the numerical calculations and the Bell-Delaware approach for the shell side of the PHB-SDCTHEX

between the shell side heat transfer coefficient in this study and the Bell-Delaware approach is around 8.6%, and, this difference is about 2.8% for the shell side pressure drop. Similarly, in Figure 4, the maximum deviation for the (PHB-SDCTHEX) is approximately 8.9% and 2.5% for shell side heat transfer coefficient and the shell side pressure drop. With this comparison, it can be said that the results have acceptable accuracy.

4. RESULTS AND DISCUSSION

4. 1. Velocity and Pressure Distributions

Velocity profiles of the shell side of the SHB-SDCTHEX and the PHB-SDCTHEX are illustrated in Figures 5 and 6. Also, the so called active zones (A) and dead zones (D) are determined for both HE. Active zones have higher turbulent flow and velocity magnitude than the dead zones. Figure 5 shows that the helical flow has a higher velocity magnitude in the central zones of the shell side. This is due to the helical baffle and its section angle and dead zones, which are created far from central zones with low velocity magnitude and creates less turbulence and non-uniform flow across the shell in the SHB-SDCTHEX. Figure 6 depicts that dead zones are eliminated in the PHB-SDCTHEX, and the flow is more uniform concerning to the SHB-SDCTHEX. When the flow crosses through the orifices, it becomes more turbulent. Velocity profiles at the inlet zones for the SHB-SDCTHEX and the PHB-SDCTHEX are depicted in Figures 5(b) and 6(b). It can be found that the flow distribution is more stable and uniform at the inlet of the PHB-SDCTHEX compared with the SHB-SDCTHEX. Similarly, velocity distributions at the outlet zones for both models are shown in Figures 5(c) and 6(c). The flow distributions are also stable at the outlet zones. Pressure distributions across the shell side for the SHB-SDCTHEX and the PHB-SDCTHEX are illustrated in Figure 7. Because of the uniform distribution of flow across the shell side, the gradient of pressure for the PHB-SDCTHEX is lower than the pressure gradient for the SHB-SDCTHEX.

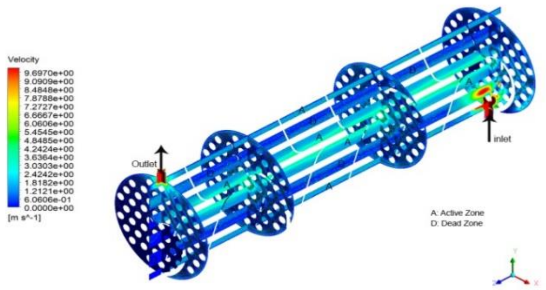

(a)

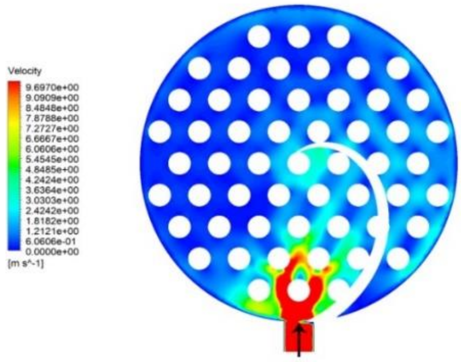

(b)

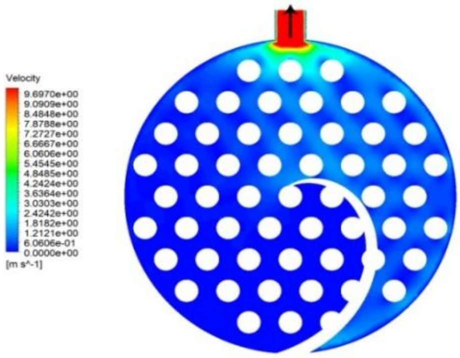

(c)

Figure 5. Velocity profiles for the SHB-SDCTHEX: (a) 3D profile (b) inlet zone (c) outlet zone with $\boldsymbol{m_s}$ = 20 ($\mathbf{kg/s}$)

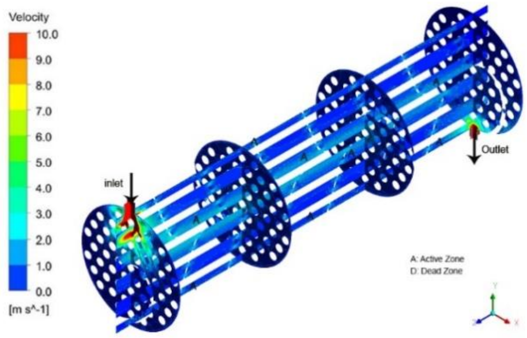

(a)

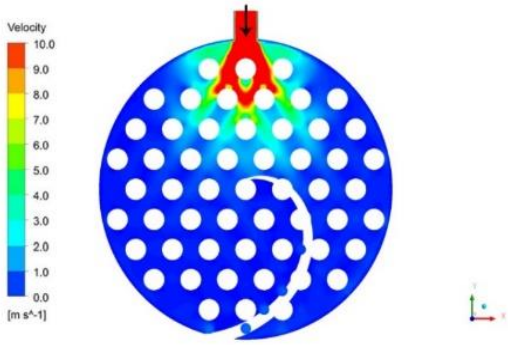

(b)

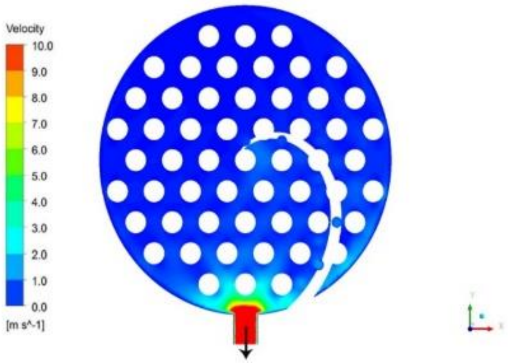

(c)

Figure 6. Velocity profiles for the PHB-SDCTHEX: (a) 3D profile (b) inlet zone (c) outlet zone with m_s = 20 (kg/s)

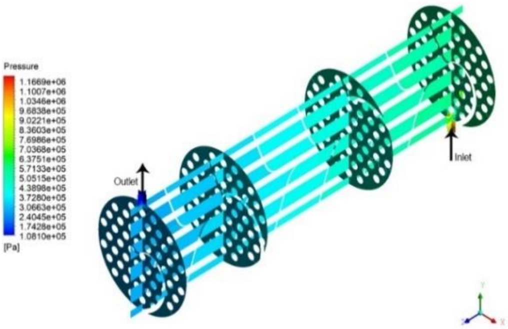

(a) (SHB-SDCTHEX)

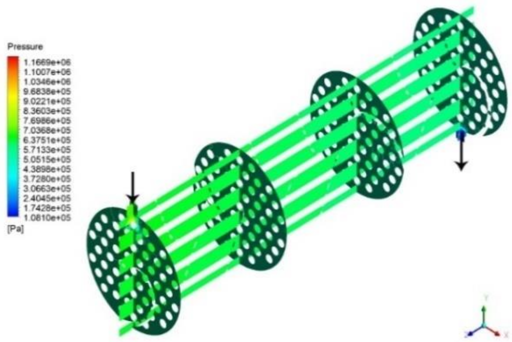

(b) (PHB-SDCTHEX)

Figure 7. Pressure distributions across the shell side: (a) for the SHB-SDCTHEX and (b) for the PHB-SDCTHEX with m_s = 20 (kg/s)

4. 2. Temperature Distributions

For the SHB-SDCTHEX and the PHB-SDCTHEX in the shell temperature distributions are depicted in Figures 8 and 9 in four various zones. Due to a simple helical baffle, with the same m_s, the outlet and inlet temperature difference on the shell side is 9.9 K and 13 K for the SHB-SDCTHEX and the PHB-SDCTHEX, respectively. As the contours illustrate, active zones (A) have a higher heat transfer coefficient than dead zones (D). The results also reveal that the local temperature in the dead zones (D) is higher than that for the active zones (A). As can be seen, the temperature distributions of the PHB-SDCTHEX are more uniform with compare to the SHB-SDCTHEX, and temperature drop happens ahead for the PHB-SDCTHEX with respect to the SHB-SDCTHEX.

4. 3. Overall Performance Comparison

To make a comparison between the performance of the SHB-SDCTHEX and the PHB-SDCTHEX, for various m_s parameters of the heat transfer rate (Q), pressure drop (ΔP), and thermo-hydraulic efficiency ($Q/\Delta P$) are used. Figure 8 shows that the heat transfer rate is enhanced for both models with an increasing mass flow rate (m_s). Increasing the value of m_s increases the amount of the convective heat transfer coefficient (h). Also, the heat transfer rate for PHB-SDCTHEX has increased by about 14.9% compared to SHB-SDCTHEX. In PHB-SDCTHEX the trend of increase of the heat transfer rate is more than that for the SHB-SDCTHEX. This is due to eliminating the dead zones by perforating the simple

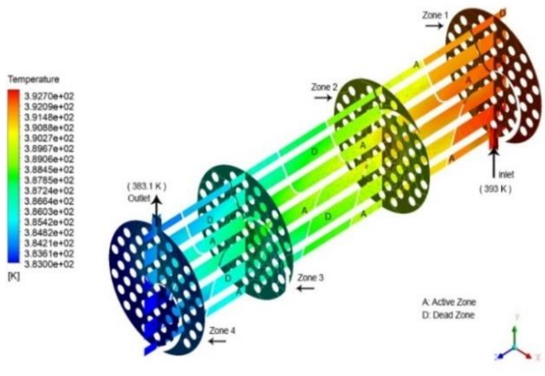

3d view

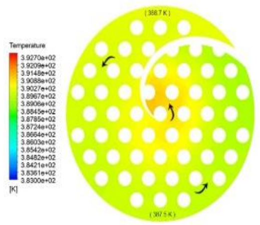

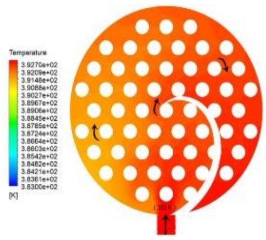

Zone 2 Zone 1

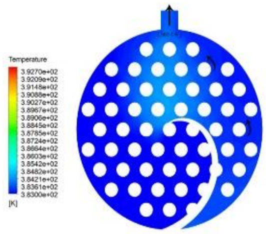

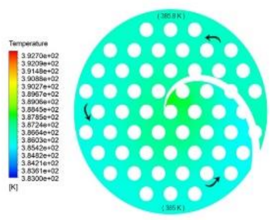

Zone 4 Zone 3

Figure 8. Temperature distribution across the shell side for the (SHB-SDCTHEX) with m_s = 20 (kg/s) in various zones

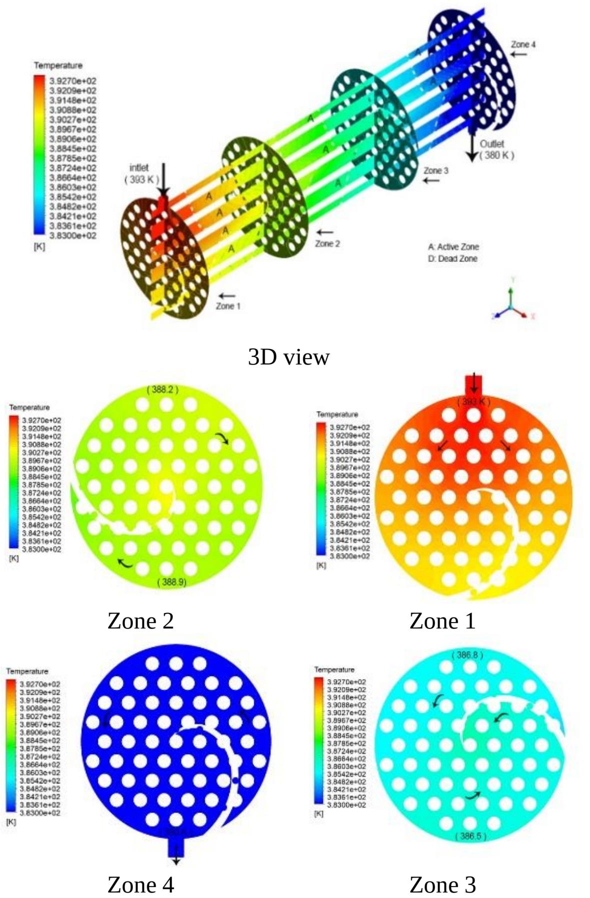

Figure 3. Temperature distribution across the shell side for the (PHB-SDCTHEX) with $\boldsymbol{m_s}$ = 20 ($\mathbf{kg/s}$) in various zones

helical baffle. Variations of the pressure drop are depicted in Figure 9. Notably, the pressure drop is an essential parameter from the cost point of view when modeling a S&T HE. The reason is that less pressure drop results in less pumping power and operating costs. Figure 9 indicates that pressure drop for the PHB-SDCTHEX is reduced by around 38.4% compared with the SHB-SDCTHEX. Also, increasing the m_s increases the pressure drop.

According to Figure 9, the growth of pressure drop for the PHB-SDCTHEX is less than that for the SHB-SDCTHEX. For evaluating the efficiency of a HE, the heat transfer rate and the pressure drop cannot be employed independently. Variations of The thermo-hydraulic performance $(Q/\Delta P)$ for both models are demonstrated in Figure 10.

It can be noticed from this figure that the $(Q/\Delta P)$ for the PHB-SDCTHEX is around 74% more than that of the SHB-SDCTHEX for the same m_s (m_s = 20 kg/s). Likewise, the $(Q/\Delta P)$ decreases with the increasing m_s. The effectiveness (ε) of a HE is expressed as follows [15]:

$$\varepsilon = \frac{Q_{av}}{Q_{max}} = \frac{Q_{av}}{(mc_p)_{min}(T_{s,in} - T_{a,in})} \tag{12}$$

In Figure 11, the pressure drop in both HEs are compared for different mass flow rates. It can be clearly seen that the pressure drop in both types of HEs increases with an increase in mass flow rate. In all flow rates, the pressure drop in SHB-SDCTHEX is always higher than PHB-SDCTHEX, and with an increase in flow rate, this difference also increases.The thermo-hydraulic performance for different values of mass flow for both HEs is shown in Figure 12. It can be seen that the maximum performance is at lower flow rates, and this parameter will decrease with an increase in flow rate of mass. Also, considering mass flow rates, the thermo-hydraulic performance of PHB-SDCTHEX is always higher than SHB-SDCTHEX, for the same flow rate. Figure 13 shows variation of the effectiveness as a function of m_s.

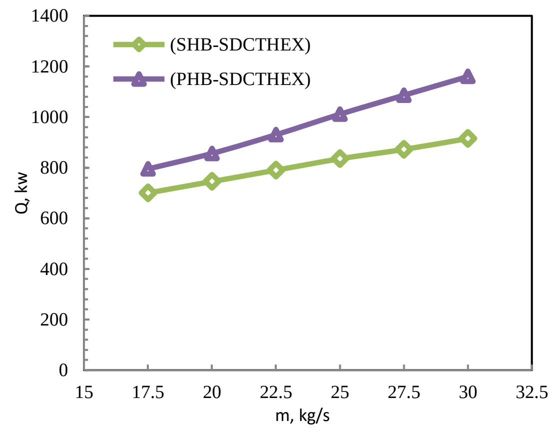

Figure 4. Variations of the heat transfer rate contrast with $\boldsymbol{m_s}$ for SHB-SDCTHEX and PHB-SDCTHEX

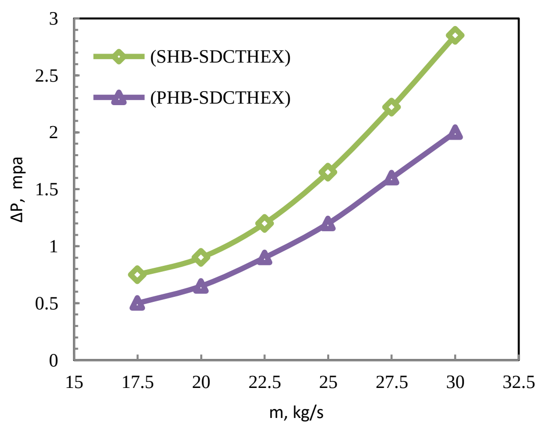

Figure 5. Variations of pressure drop contrast with $\boldsymbol{m_s}$ for SHB-SDCTHEX and PHB-SDCTHEX

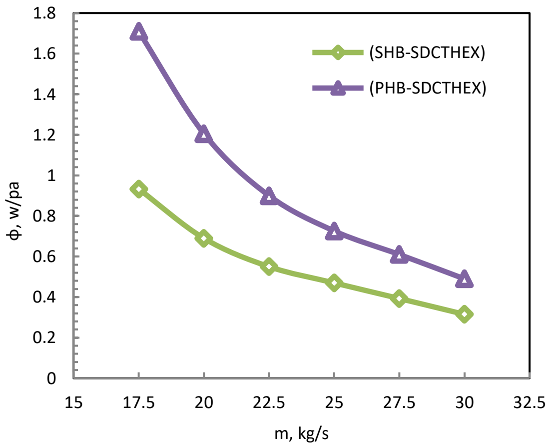

Figure 12. Variations of thermo-hydraulic performanc contrast with m_s for SHB-SDCTHEX and PHB-SDCTHEX

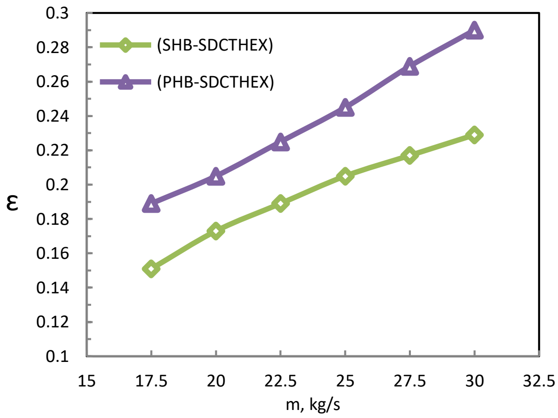

Figure 13. Variations of effectiveness contrast m_s for SHB-SDCTHEX and PHB-SDCTHEX.

Increasing m_s increases the effectiveness. For the PHB-SDCTHEX the effectiveness is around 25% more than that of the SHB-SDCTHEX. Therefore, based on the evaluation of the above parameters, the PHB-SDCTHEX is considered a convenient alternative to the SHB-SDCTHEX.

5. CONCLUSION

In this research, a shell-and-double-concentric-tube HE with a perforated helical baffle PHB-SDCTHEX is compared with a shell-and-double-concentric-tube HE with a simple helical baffle SHB-SDCTHEX using CFD. The pressure drop of the fluid flow in the shell part of this type of heat exchanger will be reduced by using the new fin used, and the heat transfer in this exchanger will significantly increase. This can be considered for the design of new converters with smaller dimensions and higher efficiency. In the following, we can point out the advantages of the serious fin compared to the simple helical fin in this type of converter as follows:

(1) Using perforated helical baffles makes the flow distribution further uniform and turbulent. Consequently, dead zones are eliminated across the shell side due to the orifices created on the simple helical baffle. It noted that the existence of the dead zones leads to a higher temperature than other zones on the shell side and less Q happens within the dead zones due to higher temperature.

(2) Q raises for the PHB-SDCTHEX around 14.9% compared with the SHB-SDCTHEX in the same conditions. It is noted that the Q increases with the increasing m_s. Also, the trend of growth of Q for the PHB-SDCTHEX is higher than that for the SHB-SDCTHEX.

(3) ΔP for the PHB-SDCTHEX decreases by about 38.4% compared with the SHB-SDCTHEX for the same m_s (m_s = 20 kg/s). Also, ΔP increases by increasing the m_s. Notably, the trend of growth of ΔP for the PHB-SDCTHEX is lower than that of the SHB-SDCTHEX.

(4) For comprehensive efficiency, the thermo-hydraulic performance ($Q/\Delta P$) and the effectiveness (ε) of the PHB-SDCTHEX are raised by about 74% and 25%, respectively; compared with the SHB-SDCTHEX for the same m_s. Likewise, ($Q/\Delta P$) is reduced by increasing the m_s. On the other hand, the effectiveness increases by increasing m_s. It should, however, be noted that most deviation of the ($Q/\Delta P$) and the (ε) in both models occurs at the minimum and maximum m_s, respectively.

6. REFERENCES

1. Sivarajan, C., Rajasekaran, B. and Krishnamohan, N., "Comparision of numerical heat transfer in conventional and helically baffled heat exchanger", ***IJERA***, Vol. 2, No. 2, (2012), 1278-1282.

2. Asgari Tahery, A., Jafarmadar, S. and Khalil Arya, S., "Hydraulic network modeling to analyze stream flow effectiveness on heat transfer performance of shell and tube heat exchangers", ***International Journal of Engineering***, ***Transactions C Aspects,*** Vol. 30, No. 6, (2017), 904-911. doi: 10.5829/ije.2017.30.06c.11.

3. Thakur, G., Singh, G., Thakur, M. and Kajla, S., "An experimental study of nanofluids operated shell and tube heat exchanger with air bubble injection", ***International Journal of Engineering, Transactions A: Basics***, Vol. 31, No. 1, (2018), 136-143. doi: 10.5829/ije.2018.31.01a.19.

4. Singh, G. and Nandan, A., "Experimental study of heat transfer rate in a shell and tube heat exchanger with air bubble injection", ***International Journal of Engineering, Transactions B: Applications***, Vol. 29, No. 8, (2016), 1160-1166. doi: 10.5829/idosi.ije.2016.29.08b.16.

5. Hosseinzadeh, K., Moghaddam, M.E., Hatami, M., Ganji, D. and Ommi, F., "Experimental and numerical study for the effect of aqueous solution on heat transfer characteristics of two phase close thermosyphon", ***International Communications in Heat and Mass Transfer***, Vol. 135, (2022), 106129. https://doi.org/10.1016/j.icheatmasstransfer.2022.106129

6. Moghaddam, M.E., Abandani, M.H.S., Hosseinzadeh, K., Shafii, M.B. and Ganji, D., "Metal foam and fin implementation into a triple concentric tube heat exchanger over melting evolution", ***Theoretical and Applied Mechanics Letters***, Vol. 12, No. 2, (2022), 100332. https://doi.org/10.1016/j.taml.2022.100332

7. Hosseinzadeh, K., Moghaddam, M.E., Asadi, A., Mogharrebi, A. and Ganji, D., "Effect of internal fins along with hybrid nano-particles on solid process in star shape triplex latent heat thermal energy storage system by numerical simulation", ***Renewable Energy***, Vol. 154, (2020), 497-507. https://doi.org/10.1016/j.renene.2020.03.054

8. Hosseinzadeh, K., Mogharrebi, A., Asadi, A., Paikar, M. and Ganji, D., "Effect of fin and hybrid nano-particles on solid process in hexagonal triplex latent heat thermal energy storage system", ***Journal of Molecular Liquids***, Vol. 300, (2020), 112347. https://doi.org/10.1016/j.molliq.2019.112347

9. Keshavarzian, B. and Sayehvand, H.-O., "Validation of the local thermal equilibrium assumption for free convection boundary layer flow over a horizontal cylinder embedded in an infinite saturated porous medium", ***Results in Physics***, Vol. 44, (2023), 106112. doi: 10.1016/j.rinp.2022.106112.

10. Keshavarzian, B. and Khosravi, M., "Numerical investigation of the structural frequencies effects on flow induced vibration and heat transfer", ***Journal of Materials and Environmental Science***, Vol. 6, No. 7, (2015), 1949-1956.

11. Keshavarzian, B., Abad, J.M.N., Mir, M., Keshavarzian, M. and Alizadeh, R., "The optimization of natural frequency on the cross flow-induced vibration and heat transfer in a circular cylinder with lstm deep learning model", ***Journal of the Taiwan Institute of Chemical Engineers***, (2023), 104969. https://doi.org/10.1016/j.jtice.2023.104969

12. Keshavarzian, B. and Sayehvand, H.-O., "Validity of the boundary layer assumptions for natural convection around a cylinder in a porous medium", ***Results in Engineering***, Vol. 18, (2023), 101069. doi: 10.1016/j.rineng.2023.101069.

13. Keshavarzian, B. and Sayehvand, H.-o., "The effect of the flow and solid matrix parameters on the nusselt number for free convection over horizontal cylinder by considering the boundary layer and local thermal non-equilibrium model", ***Journal of Thermal Analysis and Calorimetry***, (2022), 1-10. doi: 10.1007/s10973-022-11801-x.

14. Mohammadi, M., Hosseinzadeh, K. and Ganji, D.D., "Numerical analysis on the impact of axial grooves on vortex cooling behavior in gas turbine blade's leading edge", ***Proceedings of the Institution of Mechanical Engineers, Part E: Journal of Process Mechanical Engineering***, (2023), 09544089231163113. doi: 10.1177/09544089231163113.

15. Shahril, S., Quadir, G., Amin, N. and Badruddin, I.A., "Thermo hydraulic performance analysis of a shell-and-double concentric tube heat exchanger using cfd", ***International Journal of Heat and Mass Transfer***, Vol. 105, (2017), 781-798. doi: 10.1016/j.ijheatmasstransfer.2016.10.021.

16. Mukherjee, R., "Effectively design shell-and-tube heat exchangers", ***Chemical Engineering Progress***, Vol. 94, No. 2, (1998), 21-37.

17. Xianhe, D. and Songjiu, D., "Investigation of heat transfer enhancement of roughened tube bundles supported by ring or rod supports", ***Heat Transfer Engineering***, Vol. 19, No. 2, (1998), 21-27. doi: 10.1080/01457639808939917.

18. Xiao, X., Zhang, L., Li, X., Jiang, B., Yang, X. and Xia, Y., "Numerical investigation of helical baffles heat exchanger with different prandtl number fluids", ***International Journal of Heat and Mass Transfer***, Vol. 63, (2013), 434-444. doi: 10.1016/J.IJHEATMASSTRANSFER.2013.04.001.

19. Zhang, J.-F., Guo, S.-L., Li, Z.-Z., Wang, J.-P., He, Y.-L. and Tao, W.-Q., "Experimental performance comparison of shell-and-tube oil coolers with overlapped helical baffles and segmental baffles", ***Applied Thermal Engineering***, Vol. 58, No. 1-2, (2013), 336-343. doi: 10.1016/j.applthermaleng.2013.04.009.

20. Taher, F.N., Movassag, S.Z., Razmi, K. and Azar, R.T., "Baffle space impact on the performance of helical baffle shell and tube heat exchangers", ***Applied Thermal Engineering***, Vol. 44, (2012), 143-149. doi: 10.1016/j.applthermaleng.2012.03.042.

21. Picón-Núñez, M., García-Castillo, J. and Alvarado-Briones, B., "Thermo-hydraulic design of single and multi-pass helical baffle heat exchangers", ***Applied Thermal Engineering***, Vol. 105, (2016), 783-791. doi: 10.1016/J.APPLTHERMALENG.2016.04.034.

22. Shinde, S. and Chavan, U., "Numerical and experimental analysis on shell side thermo-hydraulic performance of shell and tube heat exchanger with continuous helical frp baffles", ***Thermal Science and Engineering Progress***, Vol. 5, (2018), 158-171. doi: 10.1016/J.TSEP.2017.11.006.

23. Du, T., Chen, Q., Du, W. and Cheng, L., "Performance of continuous helical baffled heat exchanger with varying elliptical tube layouts", ***International Journal of Heat and Mass Transfer***, Vol. 133, (2019), 1165-1175. doi: 10.1016/J.IJHEATMASSTRANSFER.2018.12.142.

24. Chen, J., Lu, X., Wang, Q. and Zeng, M., "Experimental investigation on thermal-hydraulic performance of a novel shell-and-tube heat exchanger with unilateral ladder type helical baffles", ***Applied Thermal Engineering***, Vol. 161, (2019), 114099. doi: 10.1016/j.applthermaleng.2019.114099.

25. Tang, H., Chen, Y., Wu, J. and Yang, S., "Numerical investigation of the performances of axial separation helical baffle heat exchangers", ***Energy Conversion and Management***, Vol. 126, (2016), 400-410. doi: 10.1016/J.ENCONMAN.2016.08.003.

26. Naqvi, S., Elfeky, K., Cao, Y. and Wang, Q., "Numerical analysis on performances of shell side in segmental baffles, helical baffles and novel clamping anti-vibration baffles with square twisted tubes shell and tube heat exchangers", ***Energy Procedia***, Vol. 158, (2019), 5770-5775. doi: 10.1016/J.EGYPRO.2019.01.553.

27. Pawar, S. and Sunnapwar, V.K., "Experimental and cfd investigation of convective heat transfer in helically coiled tube heat exchanger", ***Chemical Engineering Research and Design***, Vol. 92, No. 11, (2014), 2294-2312. doi: 10.1016/j.cherd.2014.01.016.

28. Sepehr, M., Hashemi, S.S., Rahjoo, M., Farhangmehr, V. and Alimoradi, A., "Prediction of heat transfer, pressure drop and entropy generation in shell and helically coiled finned tube heat exchangers", ***Chemical Engineering Research and Design***, Vol. 134, (2018), 277-291. doi: 10.1016/j.cherd.2018.04.010.

29. You, Y., Zhang, F., Fan, A., Dai, F., Luo, X. and Liu, W., "A numerical study on the turbulent heat transfer enhancement of rodbaffle heat exchanger with staggered tubes supported by round rods with arc cuts", ***Applied Thermal Engineering***, Vol. 76, (2015), 220-232. doi: 10.1016/J.APPLTHERMALENG.2014.11.048.

30. Liu, J., Liu, Z. and Liu, W., "3d numerical study on shell side heat transfer and flow characteristics of rod-baffle heat exchangers with spirally corrugated tubes", ***International Journal of Thermal Sciences***, Vol. 89, (2015), 34-42. doi: 10.1016/J.IJTHERMALSCI.2014.10.011.

31. Hosseinzadeh, K., Moghaddam, M.E., Asadi, A., Mogharrebi, A., Jafari, B., Hasani, M. and Ganji, D., "Effect of two different fins (longitudinal-tree like) and hybrid nano-particles (MOS_2-TiO_2) on solidification process in triplex latent heat thermal energy storage system", ***Alexandria Engineering Journal***, Vol. 60, No. 1, (2021), 1967-1979. https://doi.org/10.1016/j.aej.2020.12.001.

32. Yang, J. and Liu, W., "Numerical investigation on a novel shell-and-tube heat exchanger with plate baffles and experimental

validation", ***Energy Conversion and Management***, Vol. 101, (2015), 689-696. doi: 10.1016/J.ENCONMAN.2015.05.066.

33. Bougriou, C. and Baadache, K., "Shell-and-double concentric-tube heat exchangers", ***Heat and Mass Transfer***, Vol. 46, (2010), 315-322. doi: 10.1007/s00231-010-0572-z.

34. Lutcha, J. and Nemcansky, J., "Performance improvement of tubular heat exchangers by helical baffles", Chemical Engineering Research and Design;(UK), Vol. 68, No. A3, (1990).

35. Shah, R.K. and Sekulic, D.P., "Fundamentals of heat exchanger design, John Wiley & Sons, (2003).

36. Yang, J.-F., Zeng, M. and Wang, Q.-W., "Numerical investigation on shell-side performances of combined parallel and serial two shell-pass shell-and-tube heat exchangers with continuous helical baffles", ***Applied Energy***, Vol. 139, (2015), 163-174. doi: 10.1016/J.APENERGY.2014.11.029.

Persian Abstract

چکیده

عملکرد کلی یک مبدل حرارتی پوسته–لوله دوگانه با در نظر گرفتن فبین های ساده و مارپیچ نصب شده در قسمت پوسته، توسط نرم افزار تجاری ANSYS FLUENT 19.2 مورد بررسی قرار گرفته است. برای مقادیر مختلف دبی ورودی سیال، مقایسه جامعی برای مبدل حرارتی با فین ساده و مارپیچ صورت گرفته است. در مبدل حرارتی با فین مارپیچ نرخ انتقال حرارت، عملکرد حرارتی–هیدرولیکی مبدل و بازده مبدل به ترتیب ٢٦.٧٪، ٥٥.٥٪ و ٢٦.٦٪ بالاتر از این مقادیر برای مبدل حرارتی با فین ساده محاسبه گردید. همچنین توزیع جریان و دما در مبدل با فین های مارپیچ یکنواخت تر با تلاطم بالاتر می باشد. بنابراین، مبدل با فین های مارپیچ میتواند انتخاب بهتری برای طراحان مبدل حرارتی باشد.